Available online at www.sciencedirect.com
SCIENCE DIRECT®
Journal of Organometallic Chemistry 690 (2005) 4505–4516
Journal of Organometallic Chemistry
www.elsevier.com/locate/jorganchem

Supraphos: A supramolecular strategy to prepare bidentate ligands ☆

Joost N.H. Reek *, Marc Röder, P. Elsbeth Goudriaan, Paul C.J. Kamer, Piet W.N.M. van Leeuwen, Vincent F. Slagt

Van 't Hoff Institute for Molecular Sciences, University of Amsterdam, Nieuwe Achtergracht 166, 1018 WV Amsterdam, The Netherlands

Received 28 September 2004; received in revised form 26 January 2005; accepted 26 January 2005
Available online 18 April 2005

Abstract

Herein, we report a new strategy for the preparation of chelating bidentate ligands, which involves the mixing of two mondentate ligands functionalized with complementary binding sites. The assembly process is based on selective metal–ligand interactions employing phosphite zinc(II) porphyrins **1**–**6** and the nitrogen-containing phosphorus ligands **b**–**i** (Scheme 1). Only 14 monodentate ligands were utilized to generate a library of 48 palladium catalysts based on supraphos-type bidentate ligands. The characterization of rhodium complexes based on representative Supramolecular bidentate ligands and the comparison of their performance in the hydroformylation of styrene will be presented. The current library of catalysts was tested in the asymmetric palladium-catalyzed alkylation of *rac*-1,3-diphenyl-2-propenyl acetate, which resulted in a large variety in the observed enantioselectivity for the different catalysts. Importantly, small variations in the supraphos building blocks, lead to large differences in the enantioselectivity imposed by the catalyst, the most selective catalyst producing 97% ee.

Keywords: Catalysis; Supramolecular chemistry; Combinatorial chemistry; Palladium; Allylic substitution; Hydroformylation

1. Introduction

Bidentate chelating ligands comprise an important class of compounds for the construction of transition metal catalysts [1]. However, compared to monodentate ligands [2], the synthesis is generally more complex and time consuming. This is especially inconvenient for reactions that need intensive ligand-optimization, and as a result substantial effort has recently been devoted to the re-investigation of the potential of monodentate ligands. Although some very high enantioselectivities have been observed with monodentate ligands, there will always remain classes of reactions that require bidentate chelating ligands. Methodologies that enable the synthesis of sufficiently large libraries of bidentate phosphorus containing ligands are scarce [3], and new strategies are required to prepare diverse catalyst libraries that can be used for high throughput experimentation (HTE) [4]. Traditionally, bidentate ligands are prepared by attaching donor atoms to a ligand backbone. Herein we report a supramolecular strategy to generate bidentate ligands that involves the simple mixing of monodentate ligands [5], which is particularly suitable for combinatorial approaches and HTE [4,6]. The strategy, schematically displayed in Fig. 1, is based on the utilization of ligands functionalized with complementary binding sites. By simply mixing the ligands in solution, chelating bidentate ligands spontaneously form by assembly. In this report, we employ the commonly used axial coordination of nitrogen donor ligands to zinc(II) porphyrin building blocks as the binding motif. Breit and Seiche [7] recently reported a similar strategy to form chelating bisphos-

☆ This paper was first reported on July 7, 2004 at the XIVth International Conference on Homogeneous Catalysts in Munich/Germany.

* Corresponding author. Fax: +31 20 525 6422.
E-mail address: reek@science.uva.nl (J.N.H. Reek).

0022-328X/$ - see front matter © 2005 Elsevier B.V. All rights reserved.
doi:10.1016/j.jorganchem.2005.02.026

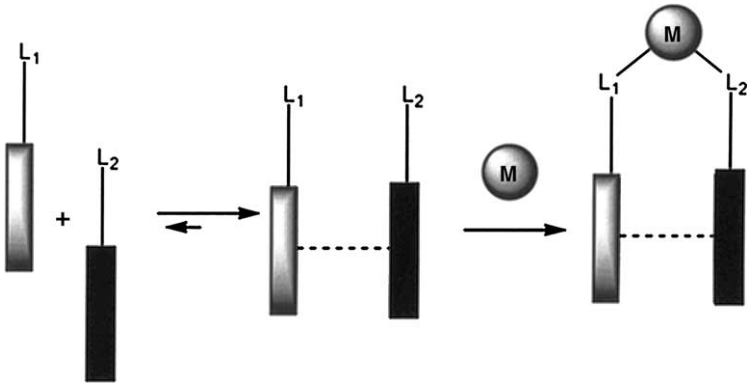

Fig. 1. A schematic representation of the supramolecular strategy to form bidentate ligands via assembly. Two ligands (L_1 and L_2) with complementary binding motifs (black and grey) will associate to form a bidentate chelating ligand.

phine ligands by the homo-assembly of two identical monodenate phosphine ligands using a self-complementary hydrogen bond motif. Interestingly, the selectivities observed for the hydroformylation of alkenes by the chelating supramolecular ligand are comparable with the best traditional covalent bidentate ligands. Takcas et al. [8] prepared a library of chiral diphosphite ligands based on phosphite functionalized chiral bisoxazoline ligands via the assembly of heteroleptic zinc complexes. The library of palladium catalysts was explored for allylic alkylation reaction and interestingly enantiomeric excesses between 20% and 99% were observed.

2. Results and discussion

We have shown previously [9] that zinc(II) porphyrins and nitrogen donor ligands offer a complementary motif that is suitable for the formation of bidentate ligands, since the binding is sufficiently strong and selective, even under conditions relevant to catalysis. For the current work we prepared six phosphite-functionalized porphyrins (**1**–**6**) that in combination with eight monodentate phosphorus ligands (**b**–**i**) generates a library of 48 chelating ligands formed by assembly (Scheme 1). The synthesis of the phosphite–porphyrins is straightforward; it involves a reaction between mono-hydroxy-zinc(II) TPP [10] (TPP = tetraphenyl porphyrin) and a phosphorochloridite [11]. The phosphite products were readily isolated after a purification over a short alumina column. Monodentate ligands **a**–**i** were commercially available or prepared via known or standard procedures (see Section 4) [12].

2.1. The assembly of phosphine–phosphite ligands and the formation of metal complexes

By simply mixing two monodentate ligands, i.e., *ortho*-phosphite zinc(II) porphyrin **1** and *meta*-pyridyldiphenylphosphine **b**, an assembled bidentate ligand **1** · **b** is formed in situ. UV–vis titrations [13,14] in toluene and NMR-spectroscopy experiments show that the pyridyl moiety of **b** selectively coordinates to zinc(II) porphyrin **1** with a binding constant of $K_{(1\cdot b)} = 1.6 \times 10^3\ M^{-1}$. The binding constant of *meta*-phosphite zinc(II) porphyrin **2** with **b** is slightly higher, $K_{(2\cdot b)} = 2.1 \times 10^3\ M^{-1}$. These results indicate that via selective pyridine–zinc interactions, two monodentate phosphorus ligands form a bidentate ligand assembly. Previously, we reported that the binding of the nitrogen donor atoms to the zinc(II) porphyrin is very selective as the phosphorus donor atoms do not coordinate to the zinc metal center and therefore they are available for transition metal coordination [9]. In order to investigate the coordination properties of this new class of ligands, their rhodium complexes were prepared and studied with high-pressure NMR spectroscopy (Table 1). The NMR-spectroscopy experiments performed in toluene-d_8 under 20 bars of H_2/CO, show that these ligand systems do indeed coordinate to transition metals in a bidentate fashion.

ortho-Phosphite zinc(II) porphyrin **1** in the presence of a rhodium precursor, [Rh(acac)(CO)$_2$], forms a monoligated rhodium phosphite complex **7**, as is the case for other bulky phosphite ligands [15]. The one-to-one mixture of 3-pyridyldiphenylphosphine **b** and **1** resulted in the generation of the assembled bidentate phosphine–phosphite ligand **1** · **b**, which results in the formation of a new bidentate phosphine–phosphite rhodium complex **8** (Scheme 2).

The rhodium–phosphorus coupling constants indicate that the assembled bidentate phosphine–phosphite ligand **1** · **b** coordinates in an equatorial–equatorial (ee) fashion to the rhodium metal center (Figs. 2 and 3). As was evident from the NMR spectra *ortho*-phosphite zinc(II) porphyrin **1** in the presence of a stoichiometric amount of triphenylphosphine **a**, yielded a mixture of two different rhodium complexes, respectively phosphine–phosphite complex **9** and a small amount of bisphosphine complex **10**. The coordination geometry of

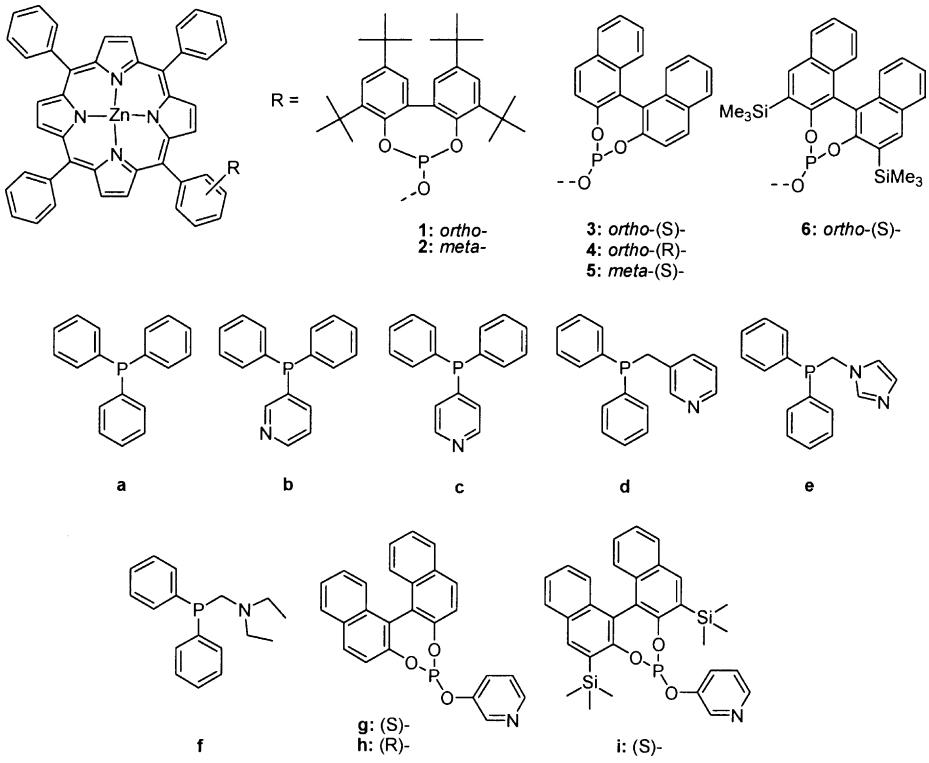

Scheme 1. Building blocks used to make bidentate supraphos ligands via assembly.

Table 1
Selected ^{1}H and ^{31}P NMR data of high-pressure NMR-spectroscopy of various rhodium complexes at $T = 25$ °C

Complex	$\delta(^{31}P)$-phosphine (ppm)	$\delta(^{31}P)$-phosphite (ppm)	J_{Rh-P} (Hz)	J_{Rh-P03} (Hz)	J_{P-PO3} (Hz)	$\delta(^{1}H)$–Rh–H (ppm)
[Rh(**1**)(acac)(CO)][a] (**7**)	[c]	127.8	[c]	300	[c]	[c]
[HRh(**1** · **b**)(CO)$_2$] (**8**)	29.4	144.3	143	265	153	−10.6
[HRh(**1**)(**a**)(CO)$_2$] (**9**)	30.1	179.8	[b]	[b]	[b]	−9.8
[HRh(**a**)$_2$(CO)$_2$] (**10**)	37.9	[c]	140	[c]	[c]	−9.1
[HRh(**2**)$_2$(CO)$_2$] (**11**)	[c]	150.4	[c]	243	[c]	−9.3
[HRh(**2** · **b**)(CO)$_2$] (**12**)	31.4	148.6	[b]	[b]	[b]	−10.8

[a] Data of the [Rh(acac)(CO)(**1**)] complex; due to its low solubility no satisfactory NMR-data were obtained for the HRh(CO)$_3$(**1**) complex.
[b] Broad signals were observed.
[c] Not present.

phosphine–phosphite complex **9** was found to be a mixture of equatorial–equatorial (ee) and equatorial–apical (ea) coordination modes which are in fast exchange on the NMR time-scale, leading to broader signals [16]. Interestingly, the addition of one equivalent of 3-pyridyldiphenylphosphine **b** to this mixture results in pyridine coordination to the zinc(II) porphyrin template of **1**, and consequently the predominant rhodium species in solution is that based on phosphine–phosphite bidentate **1** · **b** (Fig. 3).

High-pressure NMR spectra revealed that *meta*-phosphite zinc(II) porphyrin **2** in the presence of a rhodium precursor, [Rh(acac)(CO)$_2$], yields a bis-phosphite rhodium complex (**11**). The addition of 3-pyridyldiphenylphosphine **b** to this mixture also results in the formation of a bidentate phosphine–phosphite rhodium complex (**12**). The interaction of the nitrogen donor atom with the zinc(II) porphyrin is crucial for the formation of this complex, since a one-to-one mixture of **2** and triphenylphosphine **a** in the presence of rhodium does not yield a phosphine–phosphite complex, but only the bisphosphine rhodium complex **10**. These assembled bidentate ligands chelate to a transition metal in a similar fashion as their covalently linked analogues.

To obtain further proof that these assemblies indeed exhibit chelation towards transition metals UV–vis titrations (in dichloromethane) were performed to determine binding constants of the pyridine–zinc(II) porphyrin complex in the presence and absence of one equivalent of rhodium phosphine complexes. In the presence of HRh(PPh$_3$)$_3$CO, the first triphenylphosphine readily exchanges with the phosphite-ligand (**1**) due to the

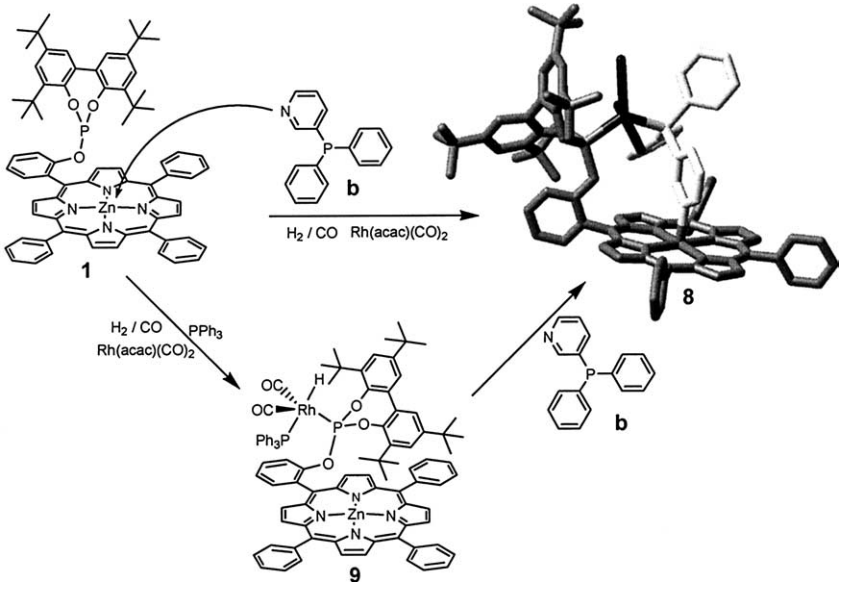

Scheme 2. Assembly of rhodium complex **8** [HRh(**1** · **b**)$(CO)_2$] (PM3 optimized structure) consisting of phosphite zinc(II) porphyrin template **1** and 3-pyridyldiphenylphosphine **b**, which can also be prepared from phosphine–phosphite complex **9** ([HRh(**1**)(**a**)$(CO)_2$]) (**a** = triprenylphosphine).

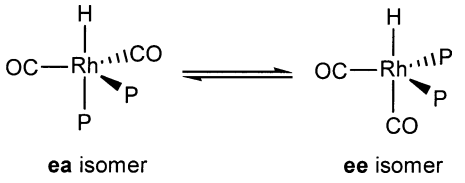

Fig. 2. Coordination modes of [HRh$(P)_2(CO)_2$]: equatorial–equatorial (ee) and equatorial–apical (ea), P = phosphorus ligand.

stronger binding properties of the phosphite. Phosphine ligand **b** competes with triphenylphosphine to coordinate to the complex, and in comparison to triphenylphosphine, ligand **b** will bind more strongly to the metal center on account of the chelate effect. The chelate energy is therefore expressed as an increase in binding energy, and if the chelate effect is negligible we expect to find similar binding constants for both experiments. UV–vis titrations of *ortho*-phosphite zinc(II) porphyrin **1** and 3-pyridyldiphenylphosphine **b** in dichloromethane indicate that the presence of a rhodium complex, [HRh$(\mathbf{a})_3$(CO)], increased the association constant by a factor of seventeen ($K = 3.8 \times 10^3\ M^{-1}$ to $K = 64.5 \times 10^3\ M^{-1}$) (Table 2), which corresponds to a 7 kJ/mol difference in binding free energies (20.5 and 27.5 kJ/mol, respectively). For *meta*-phosphite zinc(II) porphyrin **2** and **b** a similar increase was observed.

2.2. Catalysis

2.2.1. Rhodium catalyzed hydroformylation

After determining that bidentate chelating ligands can form by self-assembly, their behavior in catalysis was investigated. For this purpose we studied a selection of the assemblies for the rhodium-catalyzed hydro-

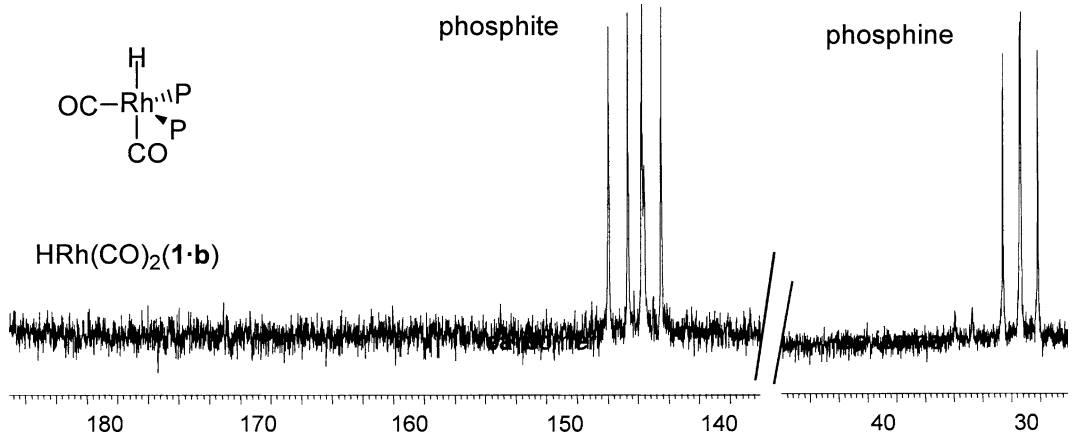

Fig. 3. High-pressure ^{31}P NMR spectrum of the assembled bidentate complex **8** [HRh(**1** · **b**)$(CO)_2$] in toluene-d_8.

Table 2
Binding constants of phosphite zinc(II) porphyrin templates and *meta*-pyridyldiphenylphosphine in dichloromethane as determined with UV–vis spectroscopy

Complex	Binding constant (K-value, M^{-1})
1 · **b**	3.8×10^3
1 · **b** + [HRh(**a**)$_3$(CO)]	64.5×10^3
2 · **b**	6.9×10^3
2 · **b** + [HRh(**a**)$_3$(CO)]	43.0×10^3

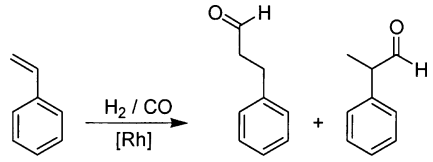

Scheme 3. The rhodium catalyzed hydroformylation of styrene.

formylation [17] of styrene (Scheme 3) and the complete library for the asymmetric allylic substitution.

The rhodium catalyzed hydroformylation of styrene was performed in toluene at 80 °C under 20 bars of H_2/CO (1/1). The results displayed in Table 3 show that key features like selectivity and activity vary considerably by using different building blocks. *ortho*-Phosphite zinc(II) porphyrin **1** yields a rhodium catalyst with high activity and low regioselectivity for the branched aldehyde in the hydroformylation of styrene (TOF = 2900 and $b/l = 2.6$). According to the complexation studies, this very bulky phosphite forms monoligated complexes, explaining the high activity. Mixing triphenylphosphine **a** and **1** yields a catalyst with a low activity and a higher b:l ratio. The [HRh(CO)$_2$(**1**)(**a**)] **9**, observed in the high-pressure NMR spectroscopy experiments, apparently undergoes catalysis with a low turn over frequency for hydroformylation. Interestingly, the assembled bidentate **1**·**b** shows a similar increase in selectivity for the branched product, but the activity of the catalyst is higher then that of complex **9**. In the mixture of the three monodentate ligands, triphenylphosphine **a**, **b** and **1** (in equal amounts), the chelating assembled bidentate ligand should predominantly coordinate to the rhodium center and indeed similar catalytic results were observed in the presence or absence of **a**. This demonstrates that the chelate species forms under reaction conditions. The *meta*-phosphite zinc (II) porphyrin **2** used as monodentate ligand results in the formation of bis-phosphite rhodium complexes (**11**), which generates reasonable activity and low selectivity in the hydroformylation of styrene (TOF = 1060 and b/l = 3.6). Ligand **2** in the presence of triphenylphosphine **a** yields predominately [HRh(CO)$_2$(**a**)$_2$] **10**, as was evident from the high-pressure NMR spectra. Consequently, a similar activity and selectivity is observed for the hydroformylation of styrene as in the absence of **2**. In contrast, upon employing the assembled bidentate ligand **2** · **b**, the activity and selectivity changes producing comparable results as observed for **1** · **b**. The addition of **a** to the solution of bidentate assembled ligand **2** · **b** does not alter the catalytic properties of the assembled rhodium complex based on **2** · **b**, again showing that the chelate effect is maintained under catalytic conditions.

Table 3
Rhodium catalyzed hydroformylation of styrene using various suprophos ligands[a]

Ligand[b]	TOF[c]	b/l[d]	Branched (%)
1	2900	2.6	72
1 + **a**	135	11.0	92
1 · **b**	398	10.4	91
1 · **b** + **a**	375	10.5	91
2	1060	3.6	78
2 + **a**	1730	5.0	83
2 · **b**	449	9.3	90
2 · **b** + **a**	461	9.4	90
a	1750	5.0	83
b	1850	5.1	83

[a] [Rh(acac)(CO)$_2$] = 0.83 mmol/l, styrene/rhodium = 12000, pressure = 20 bar (CO/H_2 = 1/1), T = 80 °C.
[b] Phosphite/rhodium = 25, phosphite/phosphine = 1.
[c] TOF = average turn over frequency = (mol aldehyde) (mol Rh)$^{-1}$ h^{-1}, the reaction was stopped after 1 h.
[d] b/l = branched/linear.

2.2.2. Palladium catalyzed allylic alkylation

The supramolecular ligand library based on monodentate phosphorus ligands **a**–**i**, and **1**–**6** was tested in the palladium catalyzed asymmetric allylic alkylation [18] of *rac*-1,3-diphenyl-2-propenyl acetate using dimethyl malonate as the nucleophile (Fig. 4). The matrix of ligands gave rise to a catalyst library of 60 members, of which 48 were based on supramolecular bidentate ligands, simply by mixing stock-solutions of the 16 monodentate ligands. In Fig. 4, the enantiomeric excess (ee) of the catalysts based on the various ligand assemblies is displayed and this figure clearly demonstrates a large variety in selectivity induced by the various members of the ligand library. For the tested catalysts, the enantiomeric excess ranged from 87% (S) to 86% (R) (Table 4). Importantly, the ee strongly depends on the ligand assembly, and both of the components are crucially important.

Unexpectedly, upon using (S)-ortho **3** as the monodentate ligand, we observed a high ee (85%, S); for this reaction only a few monodentate ligands are known to generate products with high ee's [2c,19]. In contrast, the palladium catalyst based on (S)-*meta* **5** resulted in a much lower selectivity (18% ee, S). To explain the large difference in performance, we compared the structure of the complexes based on these ligands with those based on the chiral MeO–MOP (2-diphenylphosphino-2′-methoxy-1,1′-binaphthyl) monodentate ligands of Hayashi, which also give high ee's. The solid state struc-

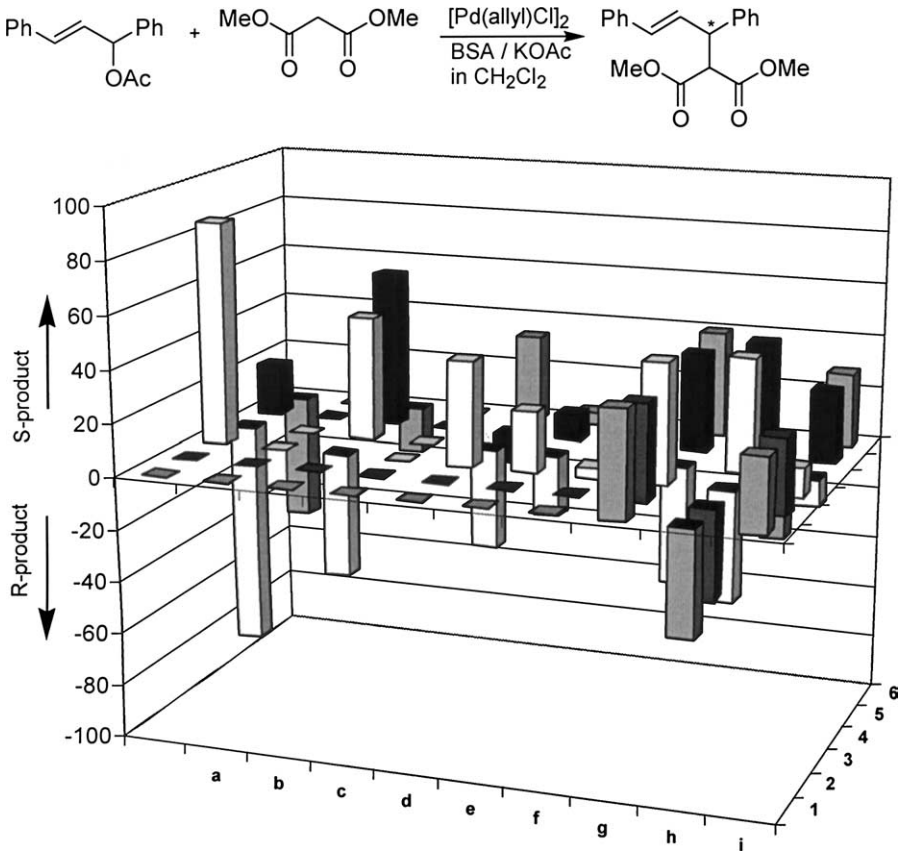

Fig. 4. Enantioselectivity results obtained for asymmetric palladium-catalyzed allylic alkylation of 1,3-diphenylallyl acetate and dimethyl malonate from a catalyst library of self-assembled bidentate ligands based on **1**–**6** and **a**–**i**.

Table 4
Allylic alkylation of 1,3-diphenylallyl acetate using different palladium catalyst assemblies at $T = -20$ °C: ee and product configuration are given[a]

Ligand	**1**	**2**	**3**	**4**	**5**	**6**
	0	0	87 (*S*)	86 (*R*)	20 (S)	48 (*R*)
a	0	0	0	0	0	0
b	0	0	47 (*R*)	47 (*S*)	59 (*S*)	17 (*R*)
c	0	0	0	0	0	0
d	0	0	40 (*S*)	38 (*R*)	11 (*R*)	33 (*S*)
e	0	0	23 (*S*)	23 (*R*)	10 (*S*)	5 (*S*)
f	0	0	4 (*S*)	3 (*R*)	22 (*R*)	0
g	40 (*S*)	36 (*S*)	45 (*S*)	45 (*R*)	37 (*S*)	40 (*S*)
h	40 (*R*)	34 (*R*)	42 (*R*)	43 (*S*)	43 (*S*)	39 (*R*)
i	28 (*S*)	28 (*S*)	11 (*S*)	10 (*R*)	27 (*S*)	28 (*S*)

[a] $[[Pd(allyl)Cl]_2] = 0.1$ mmol/l, [**1**–**6**] = 0.6 mmol/l, [**a**–**i**] = 0.6 mmol/l, the reaction was stopped after 24 h, $T = 25$ °C, complete conversion was obtained in all cases.

ture of the palladium allyl chloride complex supported by the MeO–MOP ligand shows that one of the naphthalene moieties is located close to the palladium center, which is considered to be crucial for the creation of a chiral environment [2c,20]. We have calculated the structure of the palladium allyl chloride complex with ligand **3** using PM3 calculations and we found that the porphyrin ring of this ligand is also in close proximity to the palladium center, and shielding one coordination site of the complex (Fig. 5). The calculated structure is very similar to the solid state structure of the palladium allyl chloride complex with the MeO–MOP ligand that was determined by X-ray diffraction. In addition, from the calculated structure of the complex it is evident that only one bulky ligand can coordinate to the metal. It is interesting to note that the second ligand coordinated this palladium center, which in this complex is a chloride, is only 3.8 Å from the zinc atom of the porphyrin ring. This suggests a pre-organization that facilitates the formation of the supramolecular chelating bidentate with for example **b**. In the case of (*S*)-*meta* **5** phosphite ligand, the porphyrin ring is located substantially further away from the palladium center, and this ligand is not sufficiently bulky to prevent the second ligand from coordinating to the metal center, providing a plausible explanation for the difference in selectivity obtained with ligands **3** and **5**.

Interestingly, with bidentate ligand assembly **3** · **b**, the opposite product in lower enantiomeric excess (47% ee, *R*) was obtained in contrast to monodentate **3**. In the bidentate phosphine–phosphite system, the attack of the nucleophile occurs *trans* to the phosphine

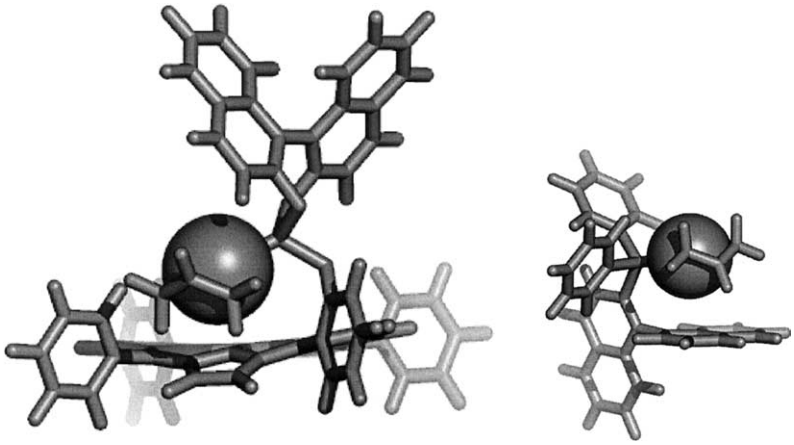

Fig. 5. PM3 optimized molecular structures of **3**Pd(allyl)Cl (left) and Pd(allyl chloride) complex with the MeO–MOP ligand (right). The palladium center, shown as CPK-model, is clearly located above the porphyrin ring in a similar fashion as previously observed for MOP ligands.

ligand [21,22], whereas in **3**Pd(allyl)Cl the attack will be *trans* to the phosphite providing an explanation for the reversal in product selectivity. Bidentate ligand assembly **5** · **b** produced a higher ee of the same product as **5** (59% ee, *S*), indicating that the formation of the chelate ligand with **b** has a completely different effect. Remarkably, bulky phosphite **6** generates preferentially the opposite enantiomeric product to that observed for the same reaction using ligand **3** (48% ee *R*). However, in the presence of co-ligand (**b**, **d**, **e**, **f**, **g**, **h**), which forms a chelating bidentate ligand, it does result in the same product as the analogous assemblies based on **3**. As expected, nonchiral **1** and **2** produced products with ee's (up to 40%) only in combination with chiral building blocks **g**–**i**. It is interesting to note that all reactions in the presence of triphenylphosphine (**a**) resulted in racemic product, indicating that the catalysis is dominated by palladium triphenylphosphine species, illustrating the importance of the presence of the nitrogen–zinc interaction to obtain chelating ligands. The introduction of two chiral centers in the supraphos-ligand, i.e., the combinations **3g**, **4g**, **5g**, **6g**, **3h**, **4h**, **5h**, **6h**, **3i**, **4i**, **5i**, **6i**, does not result in significantly higher enantioselectivities as those obtained with only one chiral center.

From the initial screening experiments some "*hits*" were identified, and these catalyst systems were subsequently studied at −20 °C (Table 5). Under these conditions the palladium catalyst supported by **3** produced products with very high enantioselectivity (97% (*S*)). The catalyst based on ligand assembly **3** · **b** gave under these conditions an enantiomeric excess of 60% (*R*). Interestingly, **3** · **b** proved to yield a more active catalyst than that based on **3**, since the yield after 24 h was 100% compared to 56%. A change in the building blocks of the supraphos ligand not only affects the selectivity but also the activity of the catalyst. At −20 °C the catalyst based on the bidentate assembly **3** · **d** resulted in the formation of the S-product with an enantiomeric excess of 44%. In analogy to previous reports of covalently linked phosphine–phosphite ligands [22], a small difference in the length of the bridge between the phosphine and phosphite resulted in a large difference in enantioselectivity. In fact, the difference between supraphos ligands **3** · **b** and **3** · **d** is only one methylene unit and for the palladium catalyzed allylic substitution of 1,3-diphenylallyl acetate this difference results in the formation of the opposite enantiomers (**3** · **b** 60% (*R*) and **3** · **d** 44% (*S*)). At −20 °C ligand **5** resulted in a catalyst that produces 42% ee (*S*), whereas the bidentate assembly **5** · **b** generates the poduct in 70% ee (*S*). In this case, the metal complex of assembly **5** · **b** is a slightly slower catalyst (40% yield compared to 73% for **5**). Importantly, small changes in the assembly of the phosphite zinc(II) porphyrin and the phosphorus ligands **a**–**i** have a large influence on the enantioselectivity as well as the activity of the catalyst system. The diversity of the relatively small supramolecular catalyst library is already sufficient to yield catalysts with selectivities ranging from 97% (*S*) to 60% (*R*).

Table 5
Allylic alkylation of 1,3-diphenylallyl acetate using different palladium catalyst assemblies at $T = -20$ °C[a]

Ligand	Conversion (%)	ee[b] (%)
3	56	97 (*S*)
3 · **b**	100	60 (*R*)
3 · **c**	100	0
3 · **d**	100	44 (*S*)
4	54	96 (*R*)
4 · **b**	100	60 (*S*)
5	73	42 (*S*)
5 · **b**	40	70 (*S*)

[a] [[Pd(allyl)Cl]$_2$] = 0.100 mmol/l, [phosphite] = 0.6 mmol/l, [phosphine] = 0.6 mmol/l, the reaction was stopped after 43 h, $T = -20$ °C.
[b] ee = enantiomeric excess.

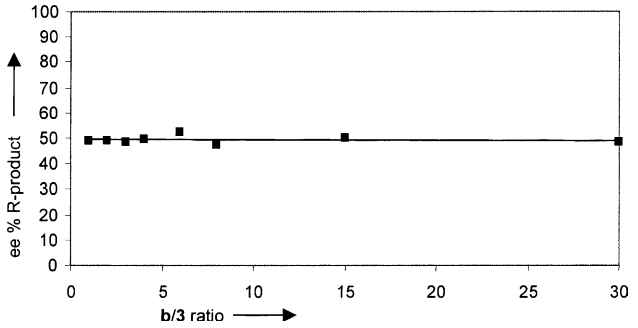

Fig. 6. Palladium catalyzed allylic alkylation at various ratios of **3**/**b** (**3**/palladium = 1) at 25 °C.

The stability of the chelating supraphos ligand was investigated in the presence of an excess of nonchiral component **b**, by monitoring the ee of the product for palladium catalyzed allylic substitution of 1,3-diphenyl-allyl acetate at various **3/b** ratios. Its clear from Fig. 6 that the enantioselectivity remains around 50% for all **b/3** ratios between 1 and 30, which in the latter case means that 90 equivalents of **b** with respect to palladium is present in the solution. This shows that under all these conditions the catalysis is dominated by the palladium complex of supraphos ligand **3** · **b**. For comparison, in all the experiments performed with triphenylphosphine (**a**, Table 4) we obtained racemic products, indicating that in these experiments the catalysis was dominated by triphenylphosphine based palladium complexes. Control experiments with supraphos **3** · **b** as the ligand in the presence and absence of triphenylphosphine produced identical results, also indicating that the chelate effect of the supraphos **3** · **b** ligand is sufficient to form exclusively **3** · **b** ligated palladium complex under these conditions.

3. Conclusion

We present here an alternative strategy for the covalent synthesis of bidentate ligands, which constitutes the assembly of two monodentate ligands with complementary binding motifs, and the new class of ligands we termed *supraphos*. In the current contribution the assembly processes are based on selective metal–ligand interactions, i.e., the axial nitrogen coordination to zinc(II) porphyrins, and we employed phosphorus based mondentate ligands. For this purpose monodentate phosphite zinc(II) porphyrin ligands **1**–**6** and phosphorus ligands **a**–**i** have been prepared. Upon mixing these monodentate ligands self-assembled bidentate ligands are formed instantaneously, as proven by NMR and UV–vis spectroscopy. Based on only 6 + 8 monodentate ligands, a catalyst library consisting of 48 bidentate assembled ligands has been prepared and was successfully employed in the palladium catalyzed asymmetric allylic alkylation. Some *hits* were identified and these promising catalyst systems generated products with high enantioselectivities up to 97% at −20 °C. In addition, it was found that small changes in the structure of the components of the assembled catalyst affected the enantioselectivity enormously. For example, the assembly of 3-pyridyldiphenylphosphine **b** and phosphite zinc(II) porphyrin **3**, preferentially leads to the formation of the *R*-product (60% ee), whereas the catalyst based on **3** gives the *S*-product in 97% ee. Importantly, the supraphos ligand **b** · **3** is tolerant towards excess of the nonchiral component **b** and triphenylphosphine, clearly demonstrating the effect of the chelate. In the control experiments with monodentate ligands the presence of triphenylphosphine resulted in racemic products. Some of the supraphos ligands were used in rhodium-catalyzed hydroformylation of styrene indicating that the class of compounds can be used for various transformations. So far we have only explored phosphite zinc(II) porphyrin **1**–**6** and the nitrogen donor ligands **a**–**i**, but many other (a)chiral building blocks can be employed for the ligand assemblies. We are currently preparing larger libraries and we are exploring other noncovalent interactions such as hydrogen bonds for their applicability to this new concept. The advantage of the approach has been clearly demonstrated as the size of the ligand library grows exponentially with the number of building blocks.

4. Experimental

4.1. General procedures

Unless stated otherwise, reactions were carried out under an atmosphere of argon using standard Schlenk techniques. THF, hexane and diethyl ether were distilled from sodium benzophenone ketyl, CH_2Cl_2, isopropanol and methanol were distilled from CaH_2 and toluene was distilled from sodium under nitrogen. NMR spectra (^1H, $^{31}P\{^1H\}$ and $^{13}C\{^1H\}$) were measured on a Bruker DRX 300 MHz and Varian Mercury 300 MHz; $CDCl_3$ was used as the solvent, if not further specified. Mass spectra were recorded on a JEOL JMS SX/SX102A four sector mass spectrometer; for FAB-MS, 3-nitrobenzyl alcohol was used as the matrix. UV–vis spectroscopy experiments were performed on a HP 8453 UV/Visible System. Elemental analyses were obtained on an Elementar Vario EL apparatus. Gas chromatographic analyses were run on an Interscience HR GC Mega 2 apparatus (split/splitless injector, J&W Scientific, DB-l J&W 30 m column, film thickness 3.0 μm, carrier gas 70 kPa He, FID Detector) equipped with a Hewlett packard Data system (Chrom-card). Chiral HPLC analyses were carried out using a Daicel Chiralcel-OD column (O.46 × 25 cm).

4.2. Materials

With exception of the compounds given below, all reagents were purchased from commercial suppliers and used without further purification. Diisopropylethylamine (dipea) and triethylamine were distilled from CaH_2 under argon. The following compounds were synthesized according to published procedures: phosphorochloridites [11], pyridylphosphines **b** and **c** [12a,b], phosphines **d**–**f** [12], hydroxyl porphyrins [10] and zinc(II) porphyrins were prepared according to the method of Adler [23].

4.2.1. Synthesis of (3,3′-5,5′-tetra-tert-butyl-1,1′-biphenyl-2,2′-diyl)(5-(phenyl-2-yl)-10,15,20-tris (phenyl) zinc(II) porphyrin) phosphite *1*

5-(2-Hydroxyphenyl)-10,15,20-tris(phenyl) zinc(II) porphyrin (1.50 g, 2.16 mmol), azeotropically dried with toluene (3 × 5 ml), and diisopropylethylamine (3.76 ml, 21.6 mmol) were dissolved in THF (80 ml) and the solution was cooled to 0 °C. Freshly prepared 3,3′-5,5′-tetra-*tert*-butyl-1,1′-biphenyl-2,2′-diyl phosphorochloridite (0.93 g, 1.96 mmol) was dissolved in THF (20 ml) and added dropwise, stirring was continued for 15 min. The cooling bath was removed and the solution was allowed to warm to room temperature, stirring was continued for 30 min. The reaction mixture was filtered and the solvent evaporated. The crude product was purified by flash column chromatography under Argon (basic alumina; CH_2C1_2) to remove the excess of hydroxyl-porphyrin, yielding **1** (1.02 g, 0.90 mmol, 46%) as a purple-red solid: ^{1}H NMR (300 MHz): δ 8.90 (m, 8H), 8.22 (m, 6H), 8.09 (m, 1H), 7.76 (m, 9H), 7.64 (m, 1H) 7.59 (m, 1H), 7.47 (m, 1H), 7.19 (d, 2H, J = 4.2 Hz), 6.93 (d, 2H, J = 4.2 Hz), 1.21 (s, 18H), 0.93 (s, 18H); ^{31}P NMR (121.5 MHz): δ 133.4; ^{13}C-ATP (75.465 MHz): δ 150.67, 150.41, 150.32, 146.63, 145.53, 143.35, 135.89, 134.71, 132.46, 132.46, 132.05, 129.27, 127.61, 126.96, 126.72, 126.68, 122.56, 121.85, 121.07, 35.24, 31.62, 30.95; HRMS (FAB+): *m/z* Calc. for $C_{72}H_{68}N_4O_3PZn$ ([MH$^+$]): 1131.4320; Obsd.: 1131.4314. Anal. Calc. for $C_{72}H_{67}N_4O_3PZn$: C, 76.35; H, 5.96; N, 4.95. Found: C, 76.26; H, 6. 15; N, 5.06%.

4.2.2. Synthesis of (3,3′-5,5′-tetra-tert-butyl-1,1′-biphenyl-2,2′-diyl)(5-(phenyl-3-yl)-10,15,20-tris (phenyl) zinc(II) porphyrin) phosphite *2*

This compound was prepared as described for **1**, using 5-(3-hydrophenyl)-10,15,20-tris(phenyl) zinc(II) porphyrin. Yield (47%) as a purple-red solid: ^{1}H NMR (300 MHz): δ 8.96–8.94 (m, 8H), 8.25–8.20 (m, 6H), 8.01 (s, 1H), 7.95 (d, 1H, J = 8.7 Hz), 7.82–7.77 (m, 9H), 7.67–7.62 (m, 1H), 7.49–7.45 (m, 1H), 7.42 (s, 2H), 7.23 (s, 2H), 1.50–1.47 (m, 18H), 1.36–1.32 (s, 18H); ^{31}P NMR (121.5 MHz): δ 139.02; ^{13}C-ATP (75.465 MHz): 150.77, 150.48, 150.22, 146.98, 144.66, 143.04, 140.42, 137.02, 136.09, 134.67, 133.07, 132.23, 130.68, 129.12, 128.45, 127.75, 126.80, 125.54, 125.07, 124.60, 122.56, 122.39, 122.13, 121.41, 119.73, 35.68, 34.85, 31.70, 31.47; HRMS (FAB+): *m/z* Calc. for $C_{72}H_{68}N_4O_3PZn$ ([MH$^+$]): 1131.4321; Obsd.: 1131.4329. Anal. Calc. for $C_{72}H_{67}N_4O_3PZn$: C, 76.35; H, 5.96; N, 4.95. Found: C, 76.83; H, 6.35; N, 4.68%.

4.2.3. Synthesis of (S)(1,1′-binaphthyl-2,2′-diyl)(5-(phenyl-2-yl)-10,15,20-tris(phenyl) zinc(II) porphyrin) phosphite *3*

5-(2-Hydroxyphenyl)-10,15,20-tris(phenyl) zinc(II) porphyrin (1.59 g, 2.30 mmol), azeotropically dried with toluene (3 × 5 ml), and diisopropylethylamine (4.0 ml, 23.0 mmol) were dissolved in THF (80 ml) and the solution was cooled to −40 °C. Freshly prepared (*S*)-2,2′-binaphtol phosphorochloridite (0.73 g, 2.09 mmol) was dissolved in THF (20 ml) and added dropwise, stirring was continued for 15 min. The cooling bath was removed and the solution was allowed to warm to room temperature, stirring was continued for 30 min. The reaction mixture was filtered and the solvent evaporated. The crude product was purified by flash column chromatography under Argon (basic alumina; CH_2Cl_2) to remove the excess of hydroxyl-porphyrin, giving **3** (0.887 g, 0.88 mmol, 42%) as a purple-red solid: ^{1}H NMR (300 MHz): δ 8.94 (d, 6H, J = 4.5 Hz), 8.89 (d, 1H, J = 4.5 Hz), 8.84 (d, 1H, J = 4.5 Hz), 8.23 (m, 6H), 8.13 (m, 2H), 7.77 (m, 11H), 7.66 (m, 2H), 7.55 (m, 1H), 7.16 (m, 1H), 6.91 (d, 1H, J = 8.7 Hz), 6.84 (m, 1H), 6.60 (d, 1H, J = 8.1 Hz), 6.45 (m, 2H), 6.38 (m, 1H), 5.72 (d, 1H, J = 8.7 Hz), 5.60 (d, 1H, J = 8.4 Hz); ^{31}P NMR (121.5 MHz): δ 145.15; ^{13}C-ATP (75.465 MHz): δ 150.62, 150.50, 150.22, 146.43, 145.32, 143.25, 135.79, 134.71, 132.42, 132.12, 131.50–130.22, 128.61, 127.53–126.63, 125.50, 125.21, 122.56, 121.85, 121.07; HRMS (FAB+): *m/z* Calc. for $C_{64}H_{40}N_4O_3PZn$ ([MH$^+$]): 1007.2130; Obsd.: 1007.2144. Anal. Calc. for $C_{64}H_{39}N_4O_3PZn$: C, 76.23; H, 3.90; N, 5.56. Found: C, 76.08; H, 4.16; N, 5.42%.

4.2.4. Synthesis of (R)(1,1′-binaphthyl-2,2′-diyl)(5-(phenyl-2-yl)-10,15,20-tris(phenyl) zinc(II)porphyrin)phosphite *4*

This compound was prepared as described for **3**, using freshly prepared (*R*)-2,2′-binaphtol phosphorochloridite. Yield (46%) as a purple-red solid: ^{1}H NMR (300 MHz): δ 8.94 (d, 6H, J = 4.5 Hz), 8.89 (d, 1H, J = 4.5 Hz), 8.84 (d, 1H, J = 4.5 Hz), 8.22 (m, 6H), 8.14 (m, 2H), 7.78 (m, 11H), 7.64 (m, 2H), 7.55 (m, 1H), 7.16 (m, 1H), 6.91 (d, 1H, J = 8.4 Hz), 6.84 (m, 1H), 6.60 (d, IH, J = 8.1 Hz), 6.45 (m, 2H), 6.38 (m, 1H), 5.71 (d, 1H, J = 8.7 Hz), 5.59 (d, 1H, J = 8.4 Hz); ^{31}P NMR (121.5 MHz): δ 145.13; ^{13}C-ATP (75.465 MHz): δ 150.62, 150.50, 150.22, 146.43,

145.32, 143.25, 135.79, 134.71, 132.42, 132.12, 131.50–130.22, 128.61, 127.53–126.63, 125.50, 125.21, 122.56, 121.85, 121.07; HRMS (FAB+): *m/z* Calc. for $C_{64}H_{40}N_4O_3PZn$ ([MH^+]): 1007.2130; Obsd.: 1007.2136. Anal. Calc. for $C_{64}H_{39}N_4O_3PZn$: C, 76.23; H, 3.90; N, 5.56. Found: C, 76.29; H, 4.14; N, 5.22%.

4.2.5. Synthesis of (S)(1,1′-binaphthyl-2,2′-diyl)(5-(phenyl-3-yl)-10,15,20-tris(phenyl) zinc(II) porphyrin) phosphite **5**

This compound was prepared as described for **3**, using 5-(3-hydroxyphenyl)-10,15,20-tris(phenyl) zinc(II) porphyrin and freshly prepared (*S*)-2,2′-binaphtol phosphorochloridite. Yield (39%) as a purple-red solid: ^{1}H NMR (300 MHz): δ 8.97–8.94 (m, 6H), 8.83–8.78 (m, 2H), 8.24-8.21 (m, 6H), 8.04–7.79 (m, 6H), 7.77 (s, 9H) 7.70–7.15 (m, 10H); ^{31}P NMR (121.5 MHz): δ 142.49; ^{13}C-ATP (75.465 MHz): δ 150.53 (C), 150.28 (C), 144.83 (C), 143.01 (C), 134.67 (CH), 132.39 (CH), 132.02 (CH), 131.49 (C), 131.05 (CH), 130.76 (CH), 130.23 (CH), 128.61 (CH), 127.83 (CH), 127.31 (CH), 127.26 (CH), 126.83 (CH), 126.83 (CH), 126.63 (CH), 125.50 (CH), 125.23 (CH), 121.99 (CH), 121.49 (C), 120.19 (CH); HRMS (FAB+): *m/z* Calc. for $C_{64}H_{40}O_3PZn$ ([MH^+]): 1007.2129; Obsd.: 1007.2109. Anal. Calc. for $C_{64}H_{39}N_4O_3Zn$: C, 76.23; H, 3.90; N, 5.56. Found: C, 76.36; H, 4.08; N, 5.42%.

4.2.6. Synthesis of (S)(3,3′-bis(trimethylsilyl)-1,1-binaphthyl-2,2′-diyl)(5-(phenyl-2-yl)-10,15,20-tris(phenyl) zinc(II) porphyrin) phosphite **6**

This compound was prepared as described for **3**, using freshly prepared (*S*)-3,3′-bis(trimethylsilyl)-2,2′-binaphtol phosphorochloridite. Yield (51%) as a purple-red solid: ^{1}H NMR (300 MHz): δ 9.06 (d, 2H), 8.96 (d, 2H, J = 5.4 Hz), 8.85 (d, 2H, J = 5.1 Hz), 8.83 (m, 2H), 8.66 (m, 1H), 8.49 (m, 3H), 8.23 (m, 2H), 8.12 (m, 2H), 8.02 (m, 1H), 7.94 (d, 2H, J = 5.4 Hz), 7.84–7.55 (m, 9H), 7.45 (m, 1H), 7.37 (m, 2H), 7.22–7.11 (m, 4H), 6.63 (m, 1H), 8.94 (m, 1H), 5.06 (m, 1H), 4.50 (m, 1H), 0.51 (s, 9H), 0.03 (s, 9H); ^{31}P NMR (121.5 MHz): δ 150.03; ^{13}C-ATP (75.465 MHz): δ 150.7, 150.5, 150.4, 145.4, 135.7, 134.7, 132.4, 132.1, 131.5–130.2, 128.7, 127.6–126.5, 125.4, 125.1, 122.5, 121.9, 121.1, 0.35, 0.20; HRMS (FAB+): *m/z* Calc. for $C_{70}H_{56}N_4O_3PSi_2Zn$ ([MH^+]): 1151.2930; Obsd.: 1151.2920. Anal. Calc. for $C_{70}H_{55}N_4O_3PSi_2Zn$: C, 72.92; H, 4.81; N, 4.86. Found: C, 72.96; H, 4.83; N, 4.71%.

4.2.7. Synthesis of (S)(1,1′-binaphthyl-2,2′-diyl)(3-pyridyl) phosphite **g**

3-Hydroxypyridine (1.44 g, 15.1 mmol), azeotropically dried with toluene (3 × 5 ml), and triethylamine (2.3 ml, 16 mmol) were dissolved in THF (40 ml) and the solution was cooled to −40 °C. Freshly prepared (*S*)-2,2′-binaphtol phosphorochloridite (5.3 g, 15.1 mmol) was dissolved in THF (20 ml) and added dropwise. The cooling bath was removed and the solution was allowed to warm to room temperature, stirring was continued for 1 h. The reaction mixture was filtered and the solvent evaporated. A mixture of toluene/hexane 1/3 (40 ml) was added to extract the product. After filtration the solvent was removed in vacuo, giving **g** (5.4 g, 13.2 mmol, 87%) as a white solid: ′H NMR (300 MHz): δ 8.54 (d, 1H, J = 2.4 Hz), 8.40 (d, 1H, J = 4.2 Hz), 8.02 (d, 1H, J = 8.7 Hz), 7.95 (d, 1H, J = 8.7 Hz), 7.92 (d, 2H, J = 8.7 Hz), 7.56-7.16 (m, 10H); ^{31}P NMR (121.5 MHz): δ 143.05; ^{13}C (75.465 MHz): 148.88 (d, J_{cp} = 6.1 Hz), 147.52 (d, J_{cp} = 4.8 Hz), 146.154 (d, J_{cp} = 1.4 Hz), 145.80 (s), 142.71 (d, J_{cp} = 7.3 Hz), 133.02 (s), 132.75 (s), 132.01 (s), 131.55 (s), 130.97 (s), 130.36 (s), 129.29 (s), 128.67 (d, J_{cp} = 4.8 Hz), 128.48 (s), 127.945 (s), 127.83 (s), 127.28 (s), 127.19 (s), 126.80 (s), 126.67 (s), 125.68 (s), 125.49 (s), 124.49 (s) 121.77 (s), 121.59 (s). HRMS (FAB+): *m/z* Calc. for $C_{25}H_{17}NO_3P$ ([MH^+]): 410.0946; Obsd.: 410.0952. Anal. Calc. for $C_{25}H_{16}NO_3P$: C, 73.35; H, 3.94; N, 3.42. Found: C, 73.20; H, 4.16; N, 3.25%.

4.2.8. Synthesis of (R)(1,1′-binaphthyl-2,2′-diyl)(3-pyridyl) phosphite **h**

This compound was prepared as described for **g**, using 3-hydroxypyridine and freshly prepared (*R*)-2,2′-binaphtol phosphorochloridite. Yield (78%) as a purple-red solid: ^{1}H NMR (300 MHz): δ 8.54 (d, 1H, J = 2.4 Hz), 8.40 (d, 1H, J = 4.2 Hz), 8.02 (d, 1H, J = 8.7 Hz), 7.95 (d, 1H, J = 8.7 Hz), 7.92 (d, 2H, J = 8.7 Hz), 7.56–7.16 (m, 10H); ^{31}P NMR (121.5 MHz): δ 143.05; ^{13}C-ATP (75.465 MHz): 148.88 (d, J_{cp} = 6.1 Hz), 147.52 (d, J_{cp} = 4.8 Hz), 146.84 (d, J_{cp} = 1,4 Hz), 145.80 (s), 142.71 (d, J_{cp} = 7.3 Hz), 133.02 (s), 132.75 (s), 132.01 (s), 131.55 (s), 130.97 (s), 130.36 (s), 129.29 (s), 128.67 (d, J_{cp} = 4.8 Hz), 128.48 (s), 127.945 (s), 127.83 (s), 127.28 (s), 127.19 (s), 126.80 (s), 126.67 (s), 125.68 (s), 125.49 (s), 124.49 (s) 121.77 (s), 121.59 (s). HRMS (FAB+): *m/z* Calc. for $C_{25}H_{17}NO_3P$ ([MH^+]): 410.0946; Obsd.: 410.0938. Anal. Calc. for $C_{25}H_{16}NO_3P$: C, 73.35; H, 3.94; N, 3.42. Found: C, 73.64; H, 4.38; N, 3.05%.

4.2.9. Synthesis of (S)(3,3′-bis(trimethylsilyl)-1,1′-binaphthyl-2,2′-diyl)(3-pyridyl) phosphite **i**

This compound was prepared as described for **g**, using freshly prepared (*S*)-3,3′-bis(trimethylsilyl)-2,2′-binaphtol phosphorochloridite. Yield (66%) as a white solid: ^{1}H NMR (300 MHz): δ 8.30 (d, 1H, J = 2.7 Hz), 8.27 (d, 1H, J = 5.1 Hz), 8.08 (d, 2H, J = 2.7 Hz), 7.92 (dd, 2H, J = 2.7, 8.1 Hz), 7.45–7.40 (m, 2H), 7.39–7.31 (m, 1H), 7.26–7.09 (m, 5H), 0.43 (s, 9H), 0.38 (s, 9H); ^{31}P NMR (121.5 MHz): δ 138.99; HRMS (FAB+):

m/z Calc. for $C_{31}H_{33}NO_{33}PSi_2$ ([MH^+]): 554.1737; Obsd.: 554.1725. Anal. Calc. for $C_{31}H_{32}NO_3PSi_2$: C, 67.24; H, 5.82; N, 2.53. Found: C, 67.18; H, 5.89; N, 2.42%.

4.3. Catalysis

The hydroformylation experiments were performed as follows. A stainless steel 25 ml autoclave, equipped with a teflon stirring bar, was charged with 0.42 μmol of [Rh(acac)$(CO)_2$], 10.4 μmol of phosphine and 0.017 ml of dipea in 4.0 ml of toluene. The solution was incubated for 1 under 20 bar CO/H_2 (1:1). The pressure was reduced to 1 bar and a mixture of 0.34 ml styrene and 0.17 ml of decane in 0.67 ml of toluene was added. Subsequently the CO/H_2 pressure was repressurized to 20 bar. The mixture was stirred at 80 °C, for 1 h. The autoclave was cooled down to 0 °C in ice and the pressure was reduced to 1.0 bar. A sample was taken and the conversion was checked by GC analysis of the crude product after filtration over a plug of silica to remove the catalyst.

The allylic alkylation experiments were performed as follows. Under Schlenk conditions 0.50 μmol of [Pd(allyl)Cl]$_2$, 3.0 μmol phosphite and 3.0 μmol phosphine were dissolved in 5.0 ml of CH_2C1_2 and stirred for 30 min. Respectively, 50 μmol 1,3-diphenylallylacetate, 150 μmol dimethyl malonate, 150 μmol BSA and 50 μmol decane and a pinch of KOAc were added. The mixture was stirred at 25 °C (−20 °C) and after 24 h the reaction was stopped by adding a saturated aqueous ammonium chloride solution. Subsequently, 5.0 ml of petroleum ether was added and the solution was washed once more with a saturated NH_4Cl solution. The organic phase was dried over Na_2SO_4, filtered and the conversion was determined by GC analysis. The solution was chromatographed (SiO_2; petroleum ether/CH_2Cl_2 = 1/1) to give analytically pure products [24]. Enantiomeric purities were determined by chiral HPLC (OD column, eluent 0.5% *iso*-propanol in hexane $t_R(R)$ = 33.2 min and $t_s(S)$ = 34.9 min).

4.4. High-pressure NMR-experiments

In a typical experiment, the high pressure NMR tube was filled with 30 μmol of [Rh(acac)$(CO)_2$], 75 μmol of phosphite zinc(II) porphyrin, 75 μmol phosphine and 1.5 ml of toluene-d_8. The tube was purged three times with 15 bar of CO/H_2 (1:1), pressurized to approximately 20 bar, heated to 80 °C and incubated for 1 h. Measurements were performed at 25 °C.

References

[1] (a) P.A. Chaloner, M.A. Esteruelas, F. Joo', L.A. Oro, Homogeneous hydrogenation, Kluwer, Dordrecht, 1994;
(b) J.M. Brown, in: E.N. Jacobsen, A. Pfaltz, H. Yamamoto (Eds.), Comprehensive Asymmetric Catalysis, vol. 1, Springer, Berlin, 1999 (Chapter 5.1);
(c) G.W. Parshall, S.D. Ittel, Homogeneous catalysis, Wiley, New York, 1992;
(d) P.W.N.M van Leeuwen, P.C.J. Kamer, J.N.H. Reek, P. Dierkes, Chem. Rev. 100 (2000) 2741.

[2] (a) I.V. Komarov, A. Borner, Angew. Chem., Int. Ed. 40 (2001) 1197;
(b) M. van den Berg, A.J. Minnaard, E.P. Schudde, J. van Esch, A.H.M. de Vries, J.G. de Vries, B.L. Feringa, J. Am. Chem. Soc. 122 (2000) 11539;
(c) T. Hayashi, Acc. Chem. Res. 33 (2000) 354.

[3] J.-B. Hu, G. Zhao, Z.-D. Ding, Angew. Chem., Int. Ed. 40 (2001) 1109.

[4] (a) J.P. Stambuli, S.R. Stauffer, K.H. Shaughnessy, J.F. Hartwig, J. Am. Chem. Soc. 123 (2001) 2677;
(b) R.F. Harris, A.A.J. Natio, G.T. Copeland, S.J. Miller, J. Am. Chem. Soc. 122 (2000) 11270;
(c) K.H. Shaughnessy, P. Kim, J.F. Hartwig, J. Am. Chem. Soc. 121 (1999) 2123;
(d) T.-Y. Yue, W.A. Nugent, J. Am. Chem. Soc. 124 (2002) 13692;
(e) M.T. Reetz, K.M. Kuhling, A. Deege, H. Hinrichs, D. Belder, Angew. Chem., Int. Ed. 39 (2000) 3891;
(f) M.T. Reetz, Angew. Chem., Int. Ed. 41 (2002) 1335;
(g) J.G. de Vries, A.H.M. de Vries, Eur. J. Org. Chem. (2003) 799;
(h) S.R. Stauffer, J.F. Hartwig, J. Am. Chem. Soc. 125 (2003) 6977.

[5] A part of the work has been published as a short communication V.F. Slagt, M. Röder, P.C.J. Kamer, P.W.N.M. van Leeuwen, J.N.H. Reek, J. Am. Chem. Soc. 126 (2004) 4056.

[6] (a) M.T. Reetz, T. Sell, A. Meiswinkel, G. Mehler, Angew. Chem., Int. Ed. 42 (2003) 790;
(b) M.T. Reetz, Angew. Chem., Int. Ed. 40 (2001) 284;
(c) M.T. Reetz, Angew. Chem., Int. Ed. 41 (2002) 1335;
(d) S.J. Taylor, J.P. Morken, Science 280 (1998) 267;
(e) M.B. Francis, E.N. Jacobsen, Angew. Chem., Int. Ed. 38 (1999) 937;
(f) R.H. Crabtree, Chem. Commun. (1999) 1611;
(g) M.B. Francis, T.F. Jamison, E.N. Jacobsen, Curr. Opin. Chem. Biol. 2 (1998) 422.

[7] B. Breit, W. Seiche, J. Am. Chem. Soc. 125 (2003) 6608.

[8] J.M. Takcas, D.S. Reddy, S.A. Moteki, D. Wu, H. Palencia, J. Am. Chem. Soc. 126 (2004) 4494.

[9] (a) V.F. Slagt, J.N.H. Reek, P.C.J. Kamer, P.W.N.M. van Leeuwen, Angew. Chem., Int. Ed. 40 (2001) 4271;
(b) V.F. Slagt, P.W.N.M. van Leeuwen, J.N.H. Reek, Angew. Chem., Int. Ed. 42 (2003) 5619;
(c) V.F. Slagt, P.W.N.M. van Leeuwen, J.N.H. Reek, Chem. Commun. (2003) 2474;
(d) V.F. Slagt, P.C.J. Kamer, P.W.N.M. van Leeuwen, J.N.H. Reek, J. Am. Chem. Soc. 126 (2004) 1526.

[10] (a) A.N. Cammidge, K.M. Lifsey, Tetrahedron Lett. 41 (2000) 6655;
(b) H. Fujii, T. Yoshimura, H. Kamada, Chem. Lett. (1996) 581.

[11] G.J.H. Buisman, L.A. van der Veen, A. Klootwijk, W.G.J. de Lange, P.C.J. Kamer, P.W.N.M. van Leeuwen, D. Vogt, Organometallics 16 (1997) 2929.

[12] (a) R.J. Bowen, A.C. Garner, S.J. Berners-Price, I.D. Jenkins, R.E. Sue, J. Organomet. Chem. 554 (1998) 181;
(b) A. Buhling, P.C.J. Kamer, P.W.N.M. van Leeuwen, J. Mol. Catal. A 98 (1995) 69;
(c) G.R. Newkome, Chem. Rev. 93 (1993) 2067, and references cited therein;
(d) K. Kellner, W. Hanke, J. Organomet. Chem. 326 (1987) C9–C12;

(e) K. Kellner, W. Hanke, A. Tzschach, Zeit. fur Chem. 24 (1984) 193;
(f) L. Maier, Helv. Chim. Acta 48 (1965) 1034;
(g) G. Bissky, G.-V. Roschenthaler, E. Lork, J. Barten, M. Medebielle, V. Staninets, A.A. Kolomeitsev, J. Fluorine Chem. 109 (2001) 173;
(h) 3-Pyridylmethyldiphenylphosphine and imidazol-1-yl-methyldiphenylphosphine were kindly donated by Shell Research and Technology center, Amsterdam, The Netherlands.

[13] (a) U. Michelsen, C.A. Hunter, Angew. Chem., Int. Ed. 39 (2000) 764;
(b) G. Szintay, A. Horvath, Inorg. Chem. Acta. 310 (2000) 175.

[14] P.N. Taylor, H.L. Anderson, J. Am. Chem. Soc. 121 (1999) 11538.

[15] T. Jongsma, G. Challa, P.W.N.M. van Leeuwen, J. Organomet. Chem. 421 (1991) 121.

[16] Low temperature ^{31}P NMR spectroscopy ($T = -20$ °C) of phosphine–phosphite complex 9 shows a double doublet (J_{Rh-P} = 131 Hz, J_{P-PO3} = 111 Hz) for the phosphine. This suggests that the phosphine is coordinated in the equatorial plane of the rhodium complex. At the given temperature the phosphite signal is a broad multiplet and the phosphine–phosphite coupling constant (J_{P-PO3} = 111 Hz) suggests that phosphite coordination to the rhodium is at the equatorial and apical position in fast exchange on the NMR spectroscopy time-scale. The phosphorus-signal of the phosphite is at rather low field (δ = 179.8 ppm) which is attributed to steric constraints, as is also found for several other phosphine–phosphite rhodium complexes..

[17] P.W.N.M. van Leeuwen, C. Claver (Eds.), Rhodium Catalyzed Hydroformylation, Kluwer Academic Publishers, Dordrecht, 2000.

[18] (a) J. Tsuji, Tetrahedron 42 (1986) 4361;
(b) B.M. Trost, D.L. Van Vranken, Chem. Rev. 96 (1996) 395;
(c) G. Helmchen, A. Pfaltz, Acc. Chem. Res. 33 (2000) 336;
(d) A. Pfaltz, Acc. Chem. Res. 26 (1993) 339;
(e) B.M. Trost, M.L. Crawley, Chem. Rev. 103 (2003) 2921.

[19] (a) T. Hayashi, M. Kawatsura, Chem. Commun. (1997) 561;
(b) T. Hayashi, M. Kawatsura, Y. Uozumi, J. Am. Chem. Soc. 120 (1998) 1681;
(c) Y. Hamada, N. Seto, H. Ohmori, K. Hatano, Tetrahedron Lett. 37 (1996) 7565;
(d) C.W. Edwards, M.R. Shipton, N.W. Alcock, H. Clase, M. Wills, Tetrahedron 59 (2003) 6473;
(e) V.N. Tsarev, S.E. Lyubimov, A.A. Shiryaev, S.V. Zheglov, O.G. Bondarev, V.A. Davankov, A.A. Kabro, S.K. Moiseev, V.N. Kalinin, K.N. Gavrilov, Eur. J. Org. Chem. (2004) 2214.

[20] (a) For detailed analysis of these effects see I.J.S. Fairlamb, G.C. Lloyd-Jones, Š. Vyskočil, P. Kočovský, Chem. Eur. J. 8 (2002) 4443;
(b) P. Dotta, P.G.A. Kumar, P.S. Pregosin, A. Albinati, S. Rizzato, Organometallics 22 (2003) 5345.

[21] R. Prétot, A. Pfaltz, Angew. Chem., Int. Ed. 37 (1998) 323.

[22] S. Deerenberg, H.S. Schrekker, G.P.F. van Strijdonck, P.C.J. Kamer, P.W.N.M. van Leeuwen, J. Fraanje, K. Goubitz, J. Org. Chem. 65 (2000) 4810.

[23] A.D. Adler, F.R. Longo, F. Kampas, J. Kim, J. Inorg. Nucl. Chem. 32 (1970) 2443.

[24] (a) Product characterization data were found in agreement with the reported literature, see for example: P. von Matt, O. Loiseleur, G. Koch, A. Pfaltz, C. Lefeber, T. Feucht, G. Helmchen, Tetrahedron Asymm. 5 (1994) 573;
(b) J.F. Bower, R. Jumnah, A.C. Williams, J.M.J. Williams, J. Chem. Soc., Perkin Trans. 1 (1997) 1411.